AERO REPORT 925

NAVY DEPARTMENT

THE DAVID W. TAYLOR MODEL BASIN

AERODYNAMICS LABORATORY

WASHINGTON 7, D.C.

LEADING-EDGE SPIKES TO REDUCE THE DRAG OF WINGS AT SUPERSONIC AIRSPEEDS

by

Richard M. Hartley

September 1957

NOTATION

Positive directions of axes, forces, moments, and angular displacements are shown by arrows

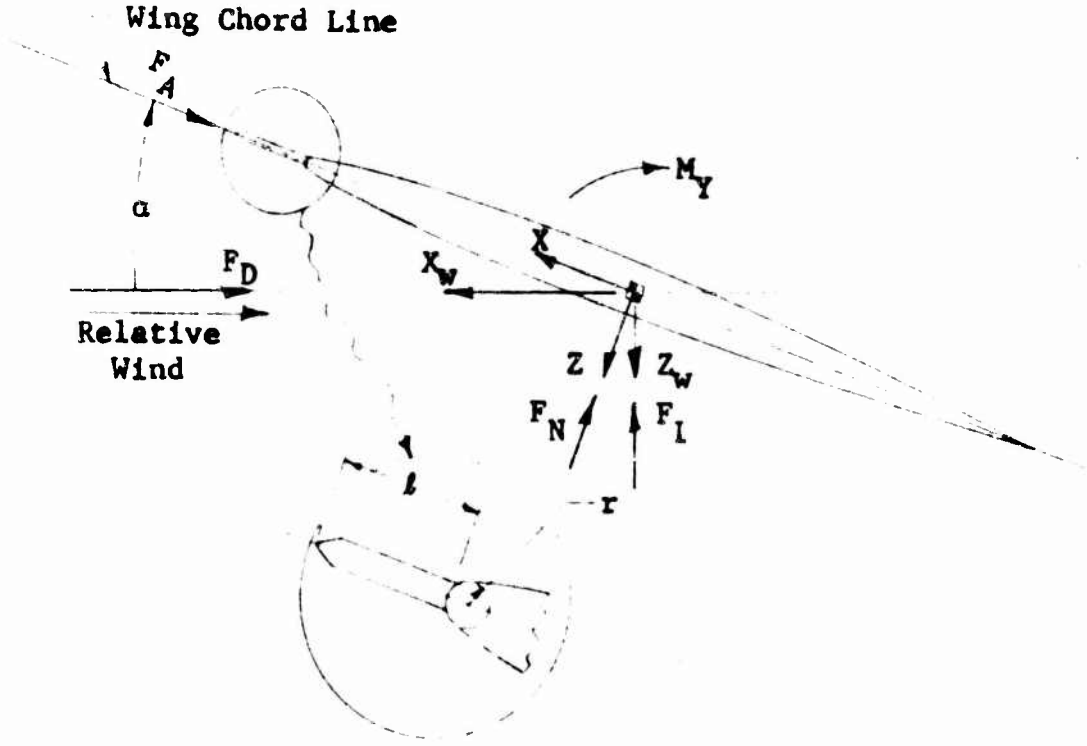

Axis	Force in pounds	Force Coefficient	Moment in pound-feet	Moment Coefficient
X	F_A	$C_A = F_A/qS$	--	--
X_w	F_D	$C_D = F_D/qS$	--	--
Y	--	--	M_Y	$C_m = M_Y/qSc$
Z	F_N	$C_N = F_N/qS$	--	--
Z_w	F_L	$C_L = F_L/qS$	--	--

Symbols

A	aspect ratio (b^2/S)
b	span
S	plan area of wing panel
c	chord of wing
r	leading-edge radius of wing
r_s	radius of spike
ℓ	spike protrusion length
q	dynamic pressure ($\gamma p M^2/2$)
V	airspeed
R	Reynolds number ($\rho Vc/\mu$)
ρ	mass density of air
μ	absolute viscosity of air
a	speed of sound in air
M	Mach number (V/a)
γ	ratio of specific heat at constant pressure to specific heat at constant volume (1.40 for air)
p	free-stream static pressure
p_t	supply (stagnation) pressure
ΔC_D	$C_{D_{(\text{wing with spikes})}} - C_{D_{(\text{wing alone})}}$

Angular Setting

α	angle of attack in degrees (angle between the wing chord plane and the relative wind vector)

TABLE OF CONTENTS

TABLE OF CONTENTS (Concluded)

Aero Report 925

AERODYNAMICS LABORATORY
DAVID TAYLOR MODEL BASIN
UNITED STATES NAVY
WASHINGTON, D. C.

LEADING-EDGE SPIKES TO REDUCE THE DRAG OF WINGS AT SUPERSONIC AIRSPEEDS

by

Richard M. Hartley

SUMMARY

A 12-percent-thick section (NACA 0012) wing panel with leading-edge spikes was tested at a Mach number of 1.88 to determine whether the wing drag could be reduced in such a manner that the ratio of maximum lift coefficient at landing speed to minimum drag coefficient at high speed would compare favorably with the ratio obtained from a thin, high-speed wing. A 6-percent-thick high-speed wing section (NACA 65-006) was tested to provide comparison data for the thick wing.

A drag reduction of 20 percent (compared to the plain wing) was obtained when spikes protruded forward ten times the leading-edge radius. This drag reduction was obtained with a spike spacing of 5 percent of the chord.

This drag reduction was not enough to make the ratio of maximum lift coefficient to minimum drag coefficient for the thick wing compare favorably with that for the thin wing. The use of high-lift devices may make the comparison more favorable, but this was not investigated.

INTRODUCTION

In a memorandum for Aerodynamics Laboratory files (Reference 1) Mr. M. J. Bamber of the Aerodynamics Laboratory,

David Taylor Model Basin suggested a method for reducing the supersonic drag of thick wings.

The method was to have spikes protrude from the leading edge of a thick wing. The spikes would produce a series of small shock waves and an initial boundary layer and thereby reduce the intensity of the leading-edge shock wave of the wing. This method is analogous to the method proposed by NACA (Reference 2) for the reduction of drag on blunt-nosed bodies.

If the drag of a thick wing could be reduced sufficiently, it could be used successfully at supersonic cruising speeds and still maintain its desirable low-speed characteristics for landing.

Tests were conducted on a wing with an NACA 0012 section at a Mach number of 1.88. Probes of various lengths and spacings were allowed to protrude from the wing leading edge. For comparison purposes, tests were also conducted on a wing of the same plan form with a high-speed airfoil section (NACA 65-006).

The models were tested in the TMB 18-inch indraft-type intermittent supersonic wind tunnel in the period from February through July 1955.

MODELS AND APPARATUS

The 6-percent-thick and 12-percent-thick wing models were manufactured of aluminum alloy at TMB. The wing models were of the semispan type and were mounted at the tunnel wall by means of a cantilever strain-gage wall balance. The cylindrical probes were inserted in holes in the wing leading edge. A maximum of 15 probes were placed on each wing. The arrangement and principal dimensions of the models are shown in Figure 1.

The probe models were made of steel drill rods. Conical and blunt-tipped probes of various lengths and diameters were used in the tests. The various probes used are shown in Figure 2.

Strain-gage outputs from the wall balance were read on Leeds and Northrup Speedomax recorders.

The supersonic airspeeds were controlled by fixed converging-diverging laval-type nozzle blocks.

TESTS

The tests were conducted in general accordance with the schedule listed in Tables 1 and 2. The angle-of-attack range was limited to approximately ±2° so that the normal force limits of the balance would not be exceeded. The low normal-force range of the balance was determined by the desired axial-force sensitivity. This angle-of-attack limitation is not undesirable since supersonic flight speeds would normally be attained only at low angles of attack.

The Reynolds numbers (based on wing chord) and air-stream supply pressures were:

Mach Number	Supply Pressure, p_t, in psi	R X 10^{-6}
1.56	13.84 to 14.46	2.66 to 3.02
1.88	14.11 to 14.46	2.25 to 2.55

The dew point of the air supply did not exceed -15°F.

RESULTS

The data are presented as dimensionless coefficients versus angle of attack and as incremental coefficients versus appropriate spike-wing geometric parameters. The axis system and coefficients used in this report are defined in the notation. The incremental values of C_D were obtained from the C_A data at $\alpha = 0°$ (where $C_A = C_D$).

ACCURACY

The data are believed to be accurate within the following limits: C_A and C_D, within ±0.0006; C_N, within ±0.004; C_m, within ±0.0005; α, within ±0.1°; M, within ±0.01; and p_o, within ±0.005 pound per square inch.

DISCUSSION

Figures 3 and 4 show the longitudinal characteristics of the 12-percent-thick and 6-percent-thick wings without leading-edge spikes.

Figures 5 and 6 show typical wing axial-force coefficients with various lengths of 0.031-inch-radius spikes added to the leading edges. In general, the addition of spikes reduces C_A. An exception to this is the slight increase of C_A for the two shortest spikes (0.2 and 0.3 inch long) on the 12-percent-thick wing. In the range where spikes produced a reduction in C_A, the reduction was greater with 15 spikes (0.05c spacing) than with 8 spikes.

Typical axial-force coefficients for wings having leading-edge spikes of varying radius are shown in Figures 7 and 8.

References 3, 4, and 5 contain experimental investigations of spikes in front of blunt-nosed bodies of revolution. The bodies tested were either ogive-cylinders with spherical tips (References 3 and 4) or a hemisphere cylinder (Reference 5). This is to say that models tested had a definite nose radius. The spikes produced drag reductions in all cases.

The spikes of References 3 and 4 were conical. The flow mechanism was deduced from schlieren photographs and is illustrated in Figure 9. Briefly, as the rod is moved forward, flow separation takes place in the vicinity of the cone-cylinder intersection. The separated-flow region trails back toward the nose in a conical shape and intersects the nose almost tangentially. The intersection is actually somewhat closer

to the body than a line tangent to the body which passes through the separation point. The process is called tip or laminar separation. This picture of the flow holds up to a certain spike protrusion. As the spike protrudes more, the flow clings to the cone-cylinder intersection and separates downstream on the cylindrical portion of the spike. The separated-flow region is again conical and streams back toward the shoulder of the nose. This process is called rod or turbulent separation. Once the transition to turbulent separation has taken place, the conical separation region does not change shape appreciably with increasing spike length.

The principal wave pattern associated with either flow consists of a conical shock wave originating from the point of the conical separation region and a curved shock wave starting from the vicinity of the intersection of the nose with the conical separation region. These two waves replace the detached wave that exists around the body in the absence of spikes.

The drag curves from four different blunt-nosed bodies of revolution are shown in Figure 10. The information comes from References 3, 4, and 5. The curves are plotted against spike length divided by nose radius (ℓ/r). References 3 and 4 show that minimum drag occurs when the flow on the spike begins to change from tip separation to spike-body separation. Minimums in the drag curves occur at ℓ/r ratios between 2 and 4 (Figure 10). Although the separation on the spikes which produce these drag minimums is a function of Reynolds number, the transition Reynolds numbers (based on spike length) in the data of Figure 10 vary through a large range. Evidently, the geometric parameter, ℓ/r, exerts a strong influence on the point of minimum drag. Specifically, minimum drag occurs in the vicinity of $\ell/r = 3$ for bodies with spherical noses at Mach numbers from 1.5 to 3.

Without spikes, the flow around the leading edge of a wing is two-dimensional except at the tip. With spikes, the flow is three-dimensional and not axially symmetric. The intersection of the conical wave from a spike with the detached leading-edge wave would be a complex shape not easily amenable to theoretical analysis. In spite of these differences, however, the drag reduction mechanism should be essentially the same as the axially symmetric case; namely, the conical wave system set up by the spikes should change the shape and thereby reduce the strength of the leading-edge detached shock wave.

In Figures 11 and 12, the drag coefficient increments at zero angle of attack are plotted versus ℓ/r, where r is the leading-edge radius of the respective wings. On the 12-percent-thick wing it can be seen that a drag coefficient reduction of approximately 0.020 occurs in the vicinity of $\ell/r = 10$ (Figure 11). The conical spikes produce greater reductions (at this ℓ/r value) than the blunt spikes. For the 6-percent wing, both the drag coefficient and percentage reduction are less than for the thicker wing (Figure 12).

The position of the undisturbed detached leading-edge wave is shown in Figures 11 and 12. This position was calculated (at zero angle of attack) by the methods of Reference 6. For the thick wing, spike lengths less than the detached wave distance produce a slight increase in drag of the wing. Once the spikes protrude beyond the detached wave, drag decreases are obtained.

Spike radius variation causes no significant change in the incremental drag coefficient for the thick wing (Figure 13). The small effect shown was caused by an unfortunate choice of spike length. For the thin wing, the incremental drag coefficients show minimums generally occurring in the range $1 < r_s/r < 2$ (Figure 14).

The spacing of spikes on the wing leading edge will have some effect on the drag reduction. Two spacings were tested: 0.10c (8 spikes per panel) and 0.05c (15 spikes per panel). The 0.05c spacing produces the greater drag reduction for both wings but the difference is small on the thick wing.

The thick wing with spikes cannot compete directly with the thin, high-speed wing on a drag basis. However, the ratio of the maximum lift coefficient at landing speed to the minimum drag at high speed is a more significant comparison quantity than merely $C_{D_{min}}$. This quantity is a speed range parameter. If the landing speed and aircraft weight are kept constant in the arguments, then this quantity is proportional to the drags of the two wings at a given high speed. This implies that a smaller wing area is used with the section that has the greater $C_{L_{max}}$.

The following table compares the characteristics of the two wings:

Characteristic	Section	
	NACA 0012 With Spikes	NACA 65-006 Without Spikes
$C_{A_{min}} = C_{D_{min}}$ (M = 1.88)	0.079	0.031
$C_{L_{max}}$ (M << 1)	0.85	0.65
$C_{L_{max}}/C_{D_{min}}$	10.8	21.0

The section characteristics of the airfoils were obtained from References 7 and 8 and the aspect ratio effects were deduced from References 9, 10, and 11. The section characteristics were obtained at a Reynolds number of 2,500,000.

The table indicates that the thin wing without spikes is still better for high-speed flight as compared to the thick wing with spikes. The comparison is made for plain wings. If auxiliary high-lift devices were contemplated (flaps, flaps with blowing, jet flaps), then the new $C_{L_{max}}$ obtained could properly be used in the $C_{L_{max}}/C_{D_{min}}$ comparison factor. The thicker wing would have an advantage in ease of installation of these devices. In the present comparison, the thick wing with spikes does not compete with the thin wing on a high-speed drag basis. However, it is possible that some other specific combination of wing, spikes, and high-lift device would allow a thick wing to compete more favorably with a thin wing. Certainly, a device that produces a 20-percent reduction in wing drag should be considered in the preliminary design phase of an airframe.

Aerodynamics Laboratory
David Taylor Model Basin
Washington, D. C.
September 1957

REFERENCES

1. MEMORANDUM FOR AERODYNAMICS LABORATORY FILES, F2 (604:MJB: sdh) of 18 Sep 1953.

2. Moeckel, W. E. Flow Separation Ahead of Blunt Bodies at Supersonic Speeds. Wash., Jul 1951. 39p. incl. illus. (National Advisory Committee for Aeronautics. TN 2418).

3. Moeckel, W. E. Flow Separation Ahead of a Blunt Axially Symmetric Body at Mach Numbers 1.76 to 2.10. Wash., Dec 1951. 12p. incl. illus. (National Advisory Committee for Aeronautics. RM E51I25).

4. Jones, Jim J. Flow Separation From Rods Ahead of Blunt Noses at Mach Number 2.72. Wash., Jul 1952. 18p. incl. illus. (National Advisory Committee for Aeronautics. RM L52E05a).

5. Jackson, Paul H., Jr. Effect of a Probe on the Drag and Pressure Distribution of a Hemispherical Nose. Pomona, Calif., Jun 1954. 30p. incl. illus. (Convair Div., General Dynamics Corp. Contract NOrd 9028) (Johns Hopkins Univ. Applied Physics Lab. CF-2140).

6. Moeckel, W. E. Approximate Method for Predicting Form and Location of Detached Shock Waves Ahead of Plane or Axially Symmetric Bodies. Wash., Jul 1949. 32p. incl. illus. (National Advisory Committee for Aeronautics. TN 1921).

7. Loftin, Laurence K., Jr. and A. H. Smith. Aerodynamic Characteristics of 15 NACA Airfoil Sections at Seven Reynolds Numbers From 0.7×10^6 to 9.0×10^6. Wash., Oct. 1949. 75p. incl. illus. (National Advisory Committee for Aeronautics. TN 1945).

8. Racisz, Stanley Frank. Effects of Independent Variations of Mach Number and Reynolds Number on the Maximum Lift Coefficients of Four NACA 6-Series Airfoil Sections. Wash., Nov 1952. 32p. incl. illus. (National Advisory Committee for Aeronautics. TN 2824).

9. Goodman, Alex and L. R. Fisher. Investigation at Low Speeds of the Effect of Aspect Ratio and Sweep on Rolling Stability Derivatives of Untapered Wings. Wash., 1950. 11p. incl illus. (National Advisory Committee for Aeronautics. Rpt 968. Formerly TN 1835, Mar 1949).

10. Jones, George W., Jr. Investigation of the Effects of Variations in the Reynolds Number Between 0.4×10^6 and 3.0×10^6 on the Low-Speed Aerodynamic Characteristics of Three Low-Aspect-Ratio Symmetrical Wings With Rectangular Plan Forms. Wash., Sep 1952. 13p. incl. illus. (National Advisory Committee for Aeronautics. RM L52 G18).

11. Johnson, Ben H., Jr. Investigation of a Thin Wing of Aspect Ratio 4 in the Ames 12-Foot Pressure Wind Tunnel. I: Characteristics of a Plain Wing. Wash., Jun 1948. 37p. incl. illus. (National Advisory Committee for Aeronautics. RM A8D07).

Table 1

Tests Conducted on 12-Percent-Thick Wing at M = 1.88

r_s = 0.031 inch

Spike Length, ℓ	Spike Spacing	
	0.10c	0.05c
0.3	C	C
0.4	B,C*	B,C*
0.6	C	C
0.8	C	B,C
1.6	C	B,C
2.0	C	C
2.4	C	C
3.2	C	C
4.0	C	C

B - Blunt tip

C - Conical tip

*Also tested with r_s = 0.047 inch

Table 2

Tests Conducted on 6-Percent-Thick Wing

(a) M = 1.88, r_s = 0.031 inch

Spike Length, ℓ	Spike Spacing	
	0.10c	0.05c
0.2	B,C	B,C
0.4	B,C*	B,C*
0.6	C	C
0.8	B,C	B,C
1.6	B	B

(b) M = 1.56, r_s = 0.031 inch

Spike Length, ℓ	Spike Spacing	
	0.10c	0.05c
0.2	B,C	B,C
0.3	B,C	B,C
0.4	B,C*	B,C*
0.6	C	C
0.8	B,C	B,C
1.6	B,C	B

B - Blunt tip

C - Conical tip

*Also tested with r_s = 0.047 and 0.062 inch

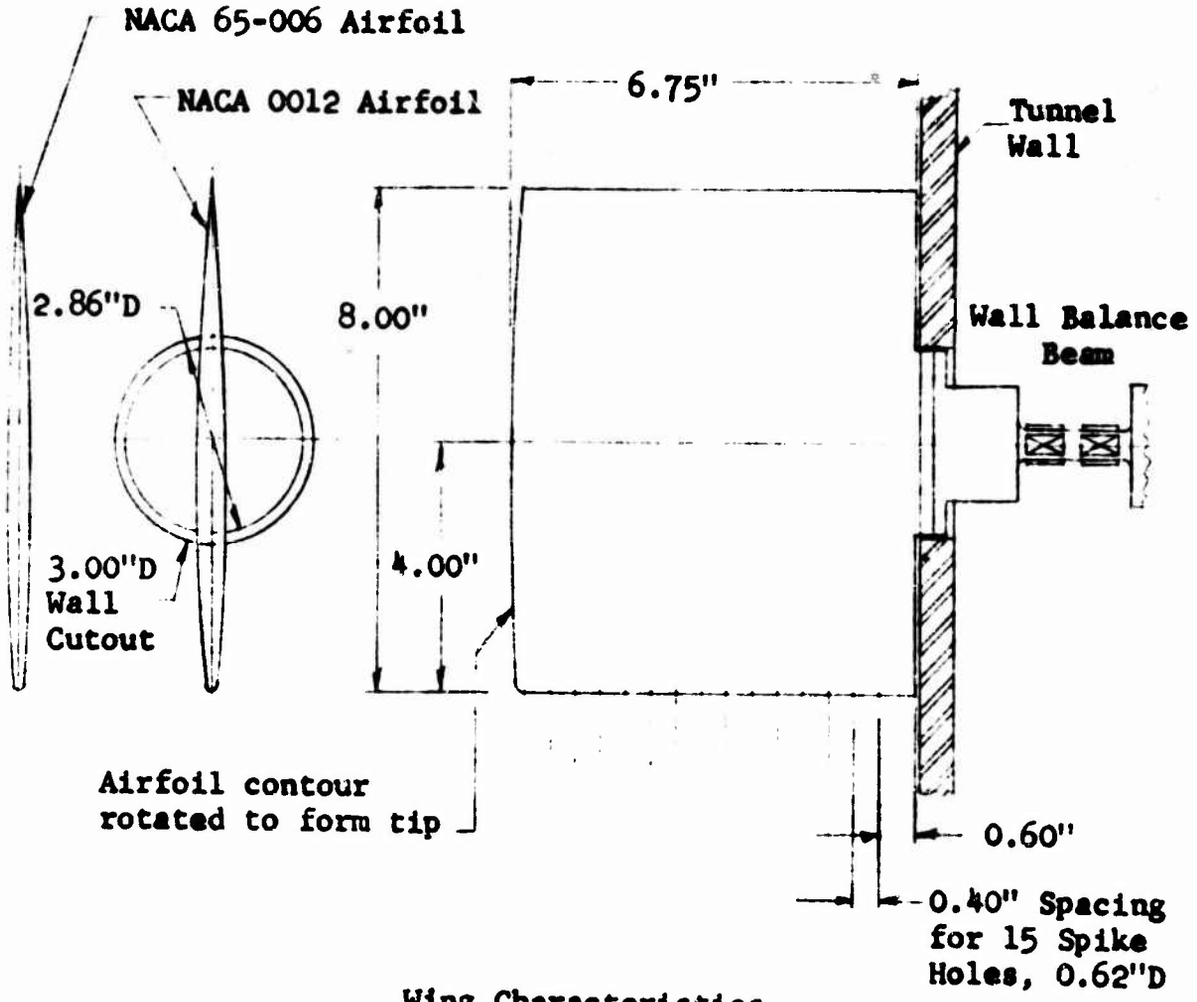

Wing Characteristics

Airfoil	NACA 0012	NACA 65-006
Semispan in inches	6.75	6.75
Chord in inches	8.00	8.00
Panel area in sq. in.	52.77	53.23
Aspect ratio	1.73	1.71
L.E. radius, r, in in.	0.126	0.030

Figure 1 - General Arrangement of Wing Panels

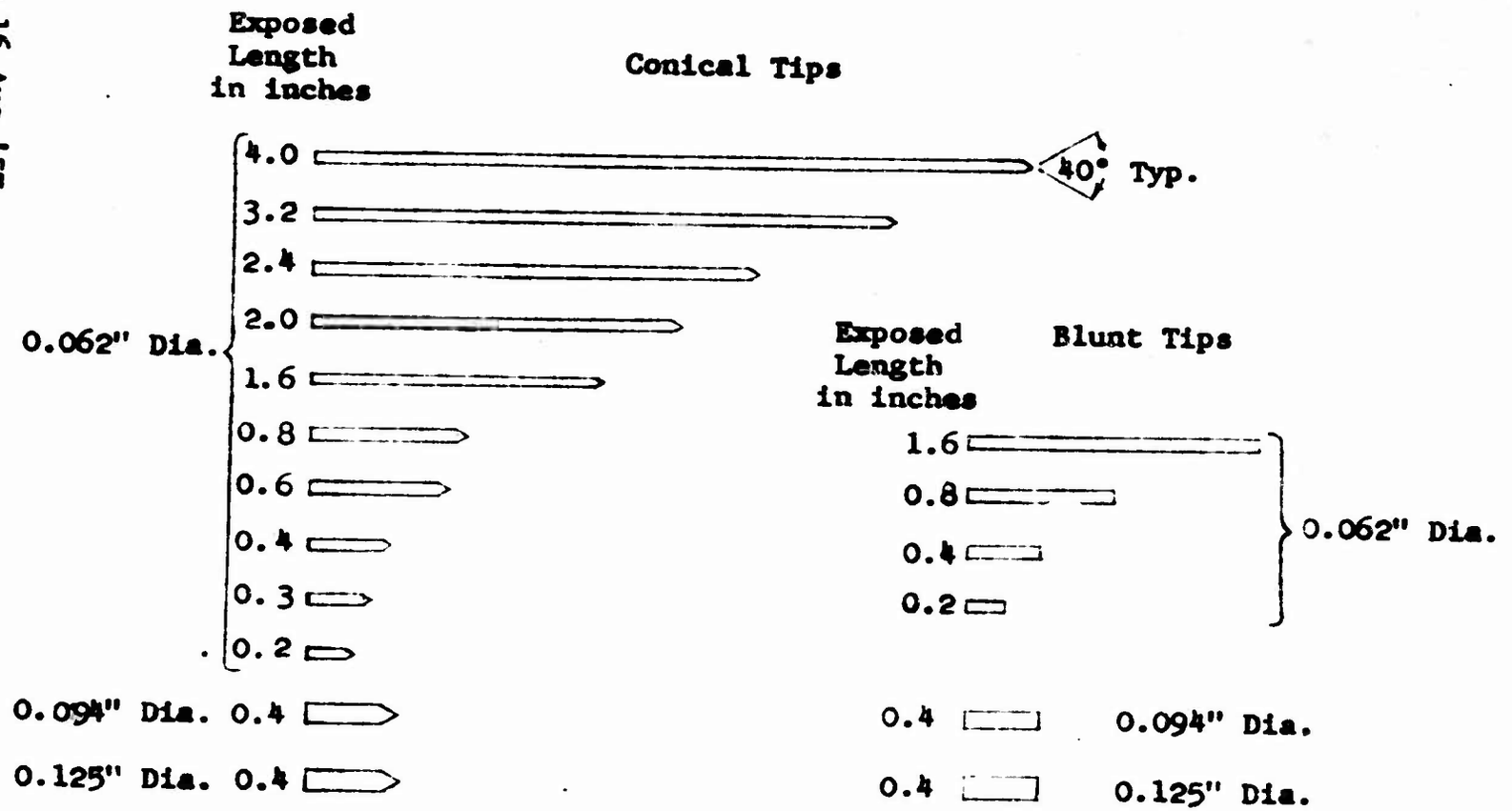

Figure 2 - Types of Spikes Tested on Wing Leading Edges

FIGURE 2

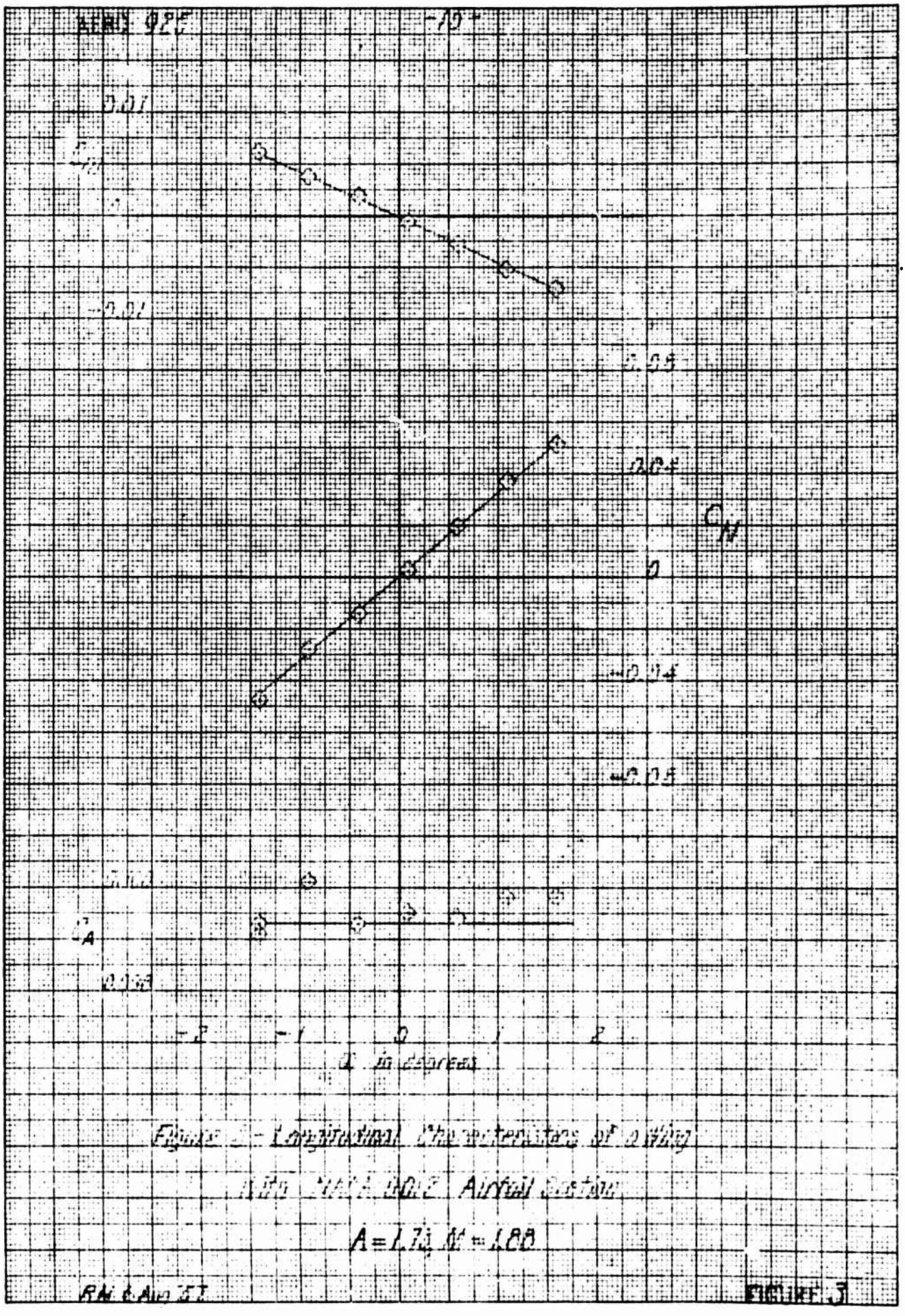

Figure 3 - Longitudinal Characteristics of Wing

with Tail and Airfoil Section

$A = 1.73$, $M = 1.88$

RM 8 AM 52

FIGURE 3

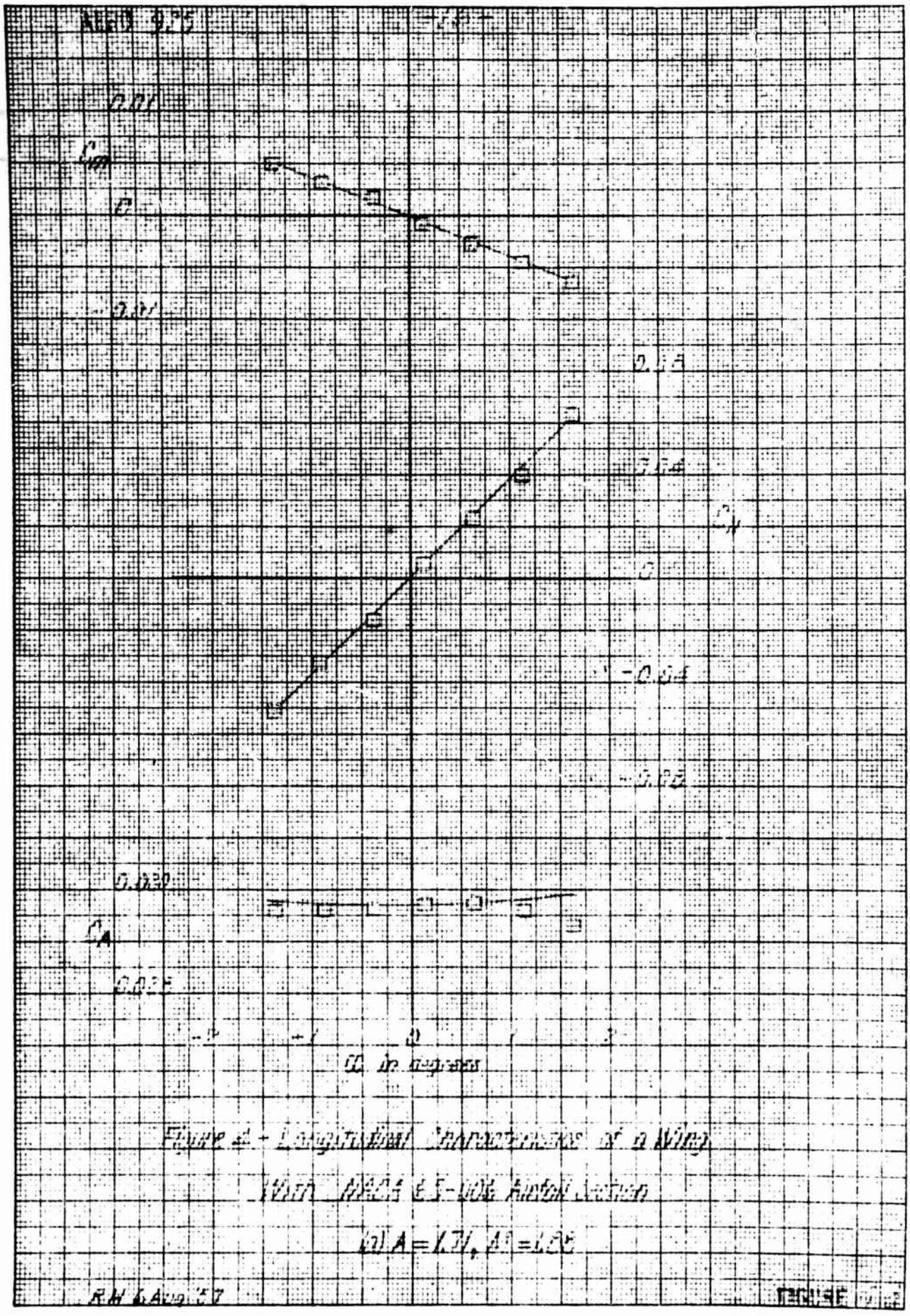

Figure 2 - Longitudinal Characteristics of a Wing
with Part of T.E. Flap Deflected
(a) $A = 4.34$, $A' = 1.86$

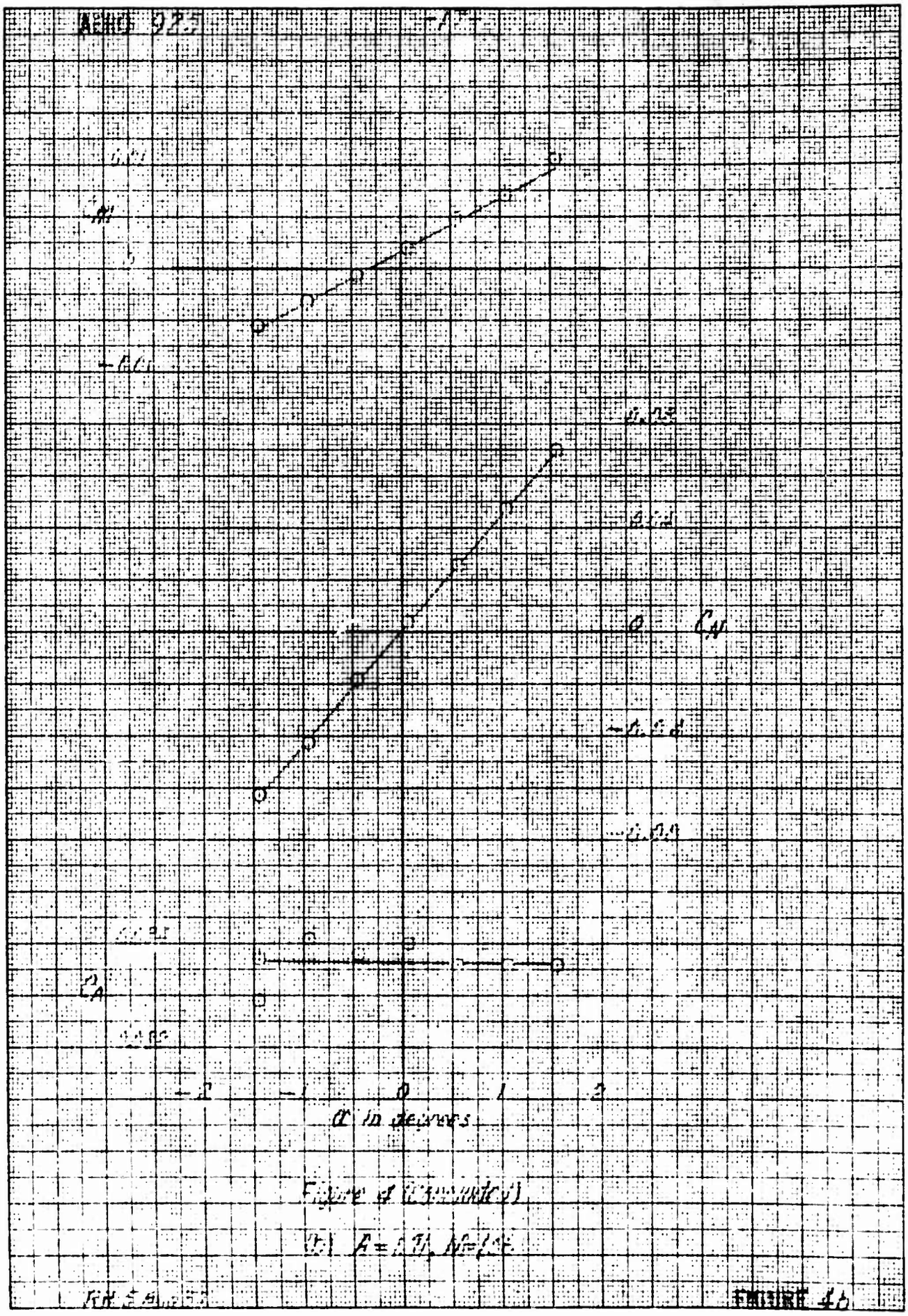
α in degrees

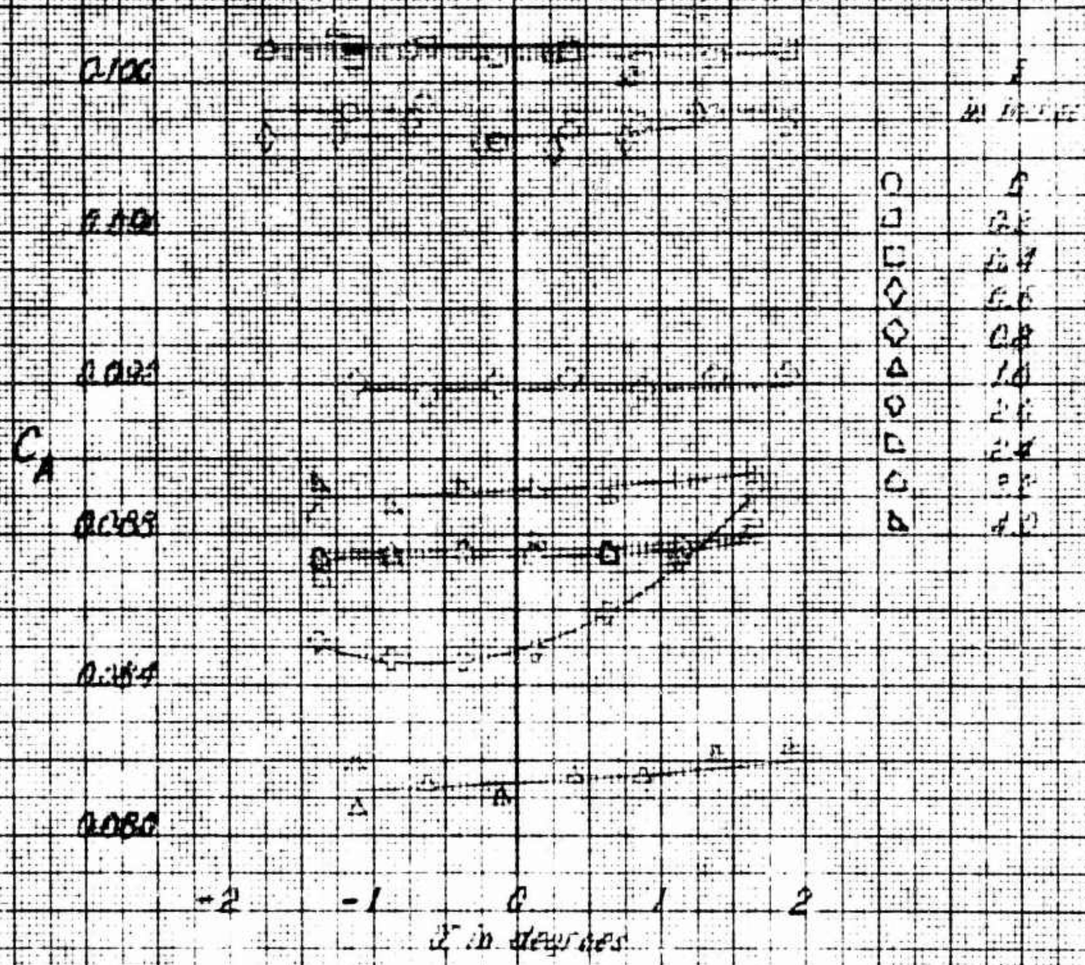

Figure 5 – Typical Effect of Spike Length on Axial-Force Coefficient for a 4-Percent-Thick Wing

M = 1.4[illegible], [illegible], [illegible], r_s = 0.0[illegible] in.

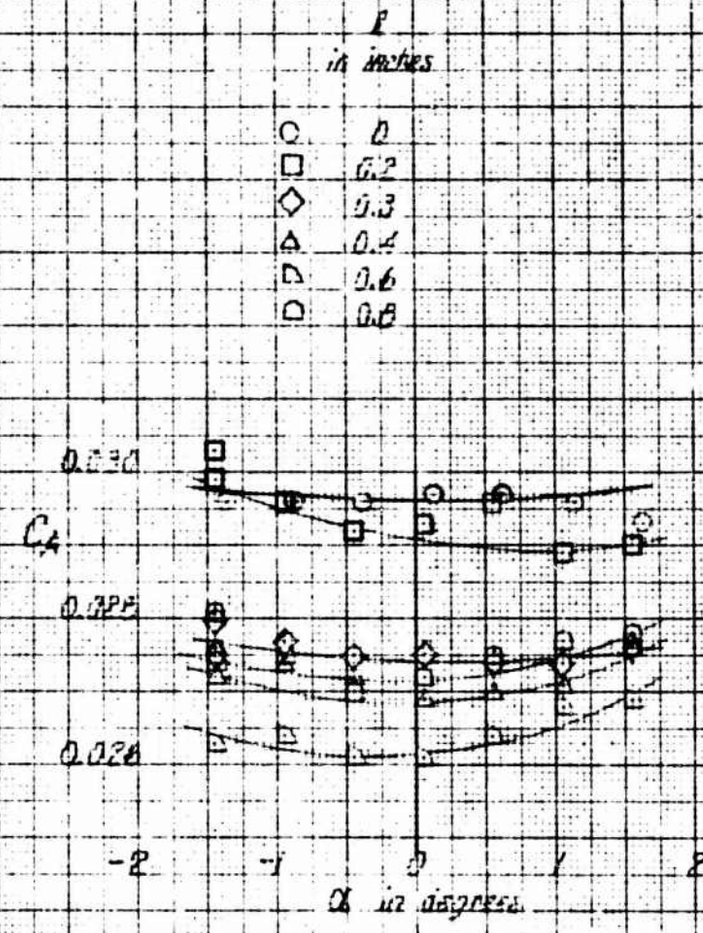

Figure 6 - Typical Effect of Spike Length on Axial-Force Coefficient for a 6-Percent-Thick Wing (at M = 1.62, Conical Spike Tip, 0.050 Spacing, r_s = 0.031 Inch)

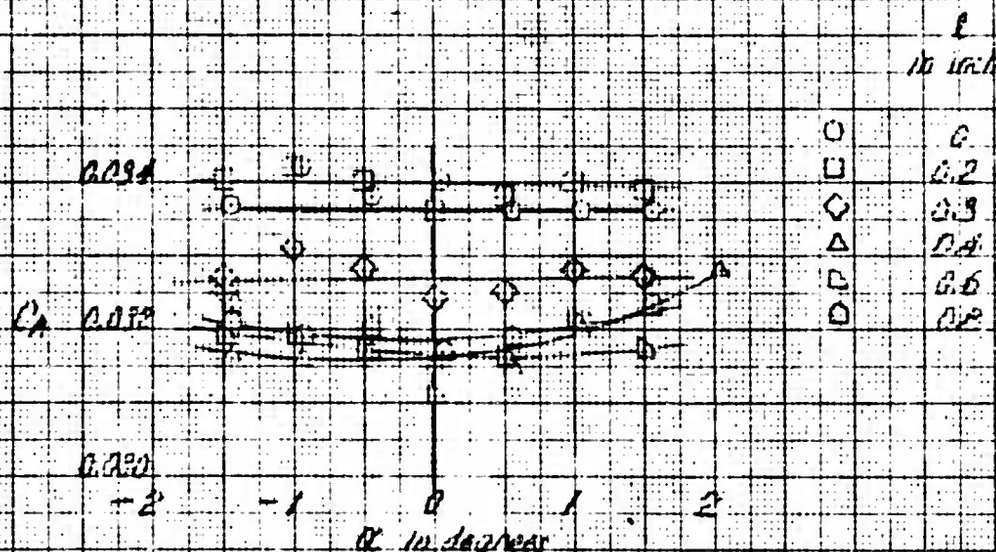

Figure 6 (Concluded)

(b) M=1.5, Conical Spike Tips, 2.05" Spacing, r_s = 0.03" Rad

FIGURE 66

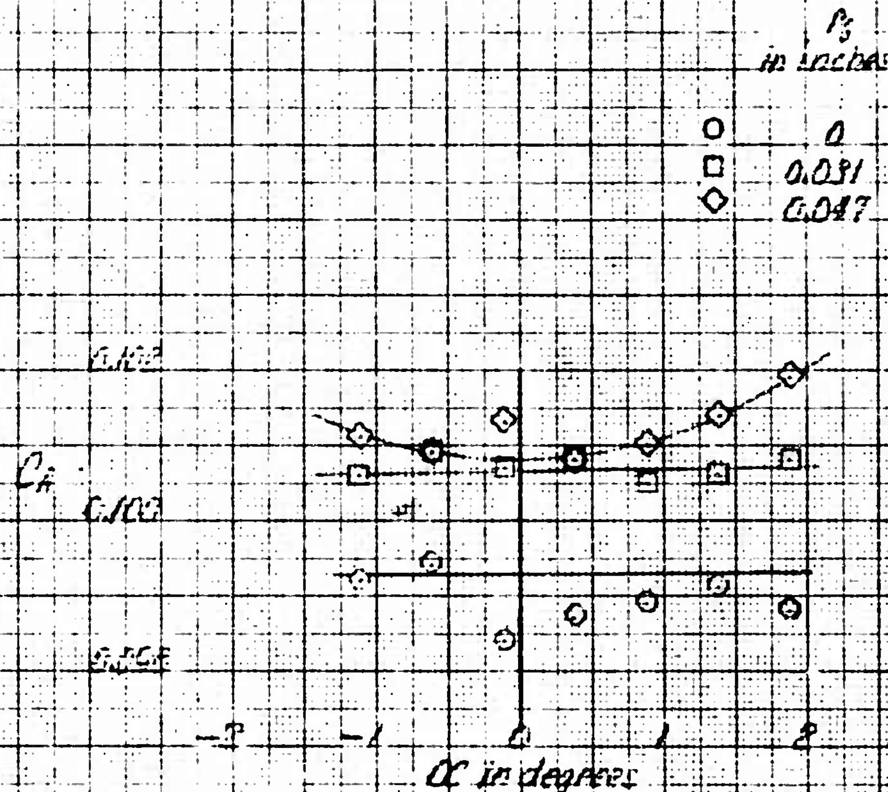

Figure 7 - Typical Effect of Spike Radius on Axial-Force Coefficient for a 12-Percent-Thick Wing

M = 1.62, Conical Spike Tips, 0.05c Spacing, l = 0.4 inch

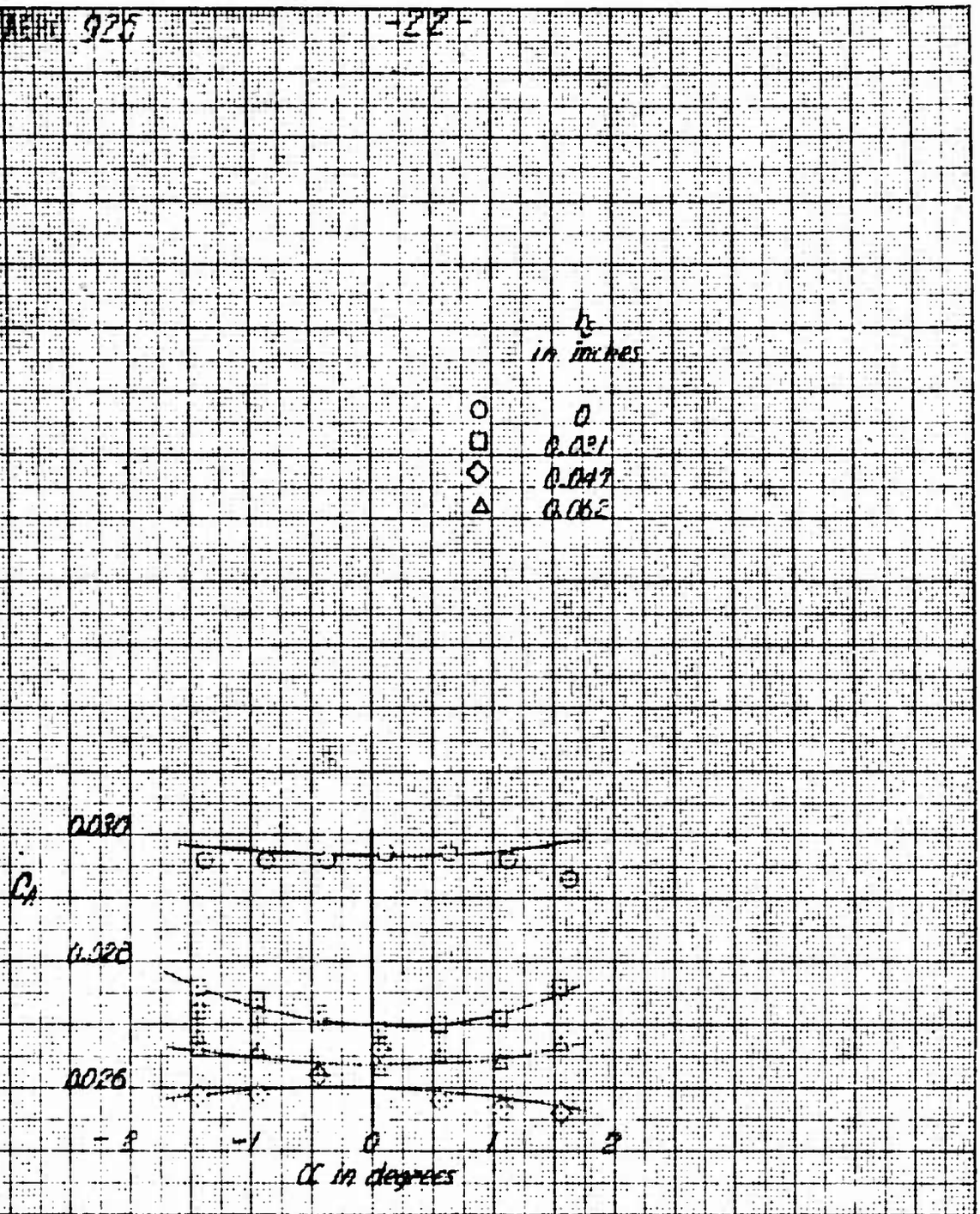

Figure 8 – Typical Effect of Spike Radius on Axial-Force Coefficient for a 6-Percent-Thick Wing (a) $M = 1.86$, Conical Spike Tips, 0.03c Spacing, $l = 0.4$ inch.

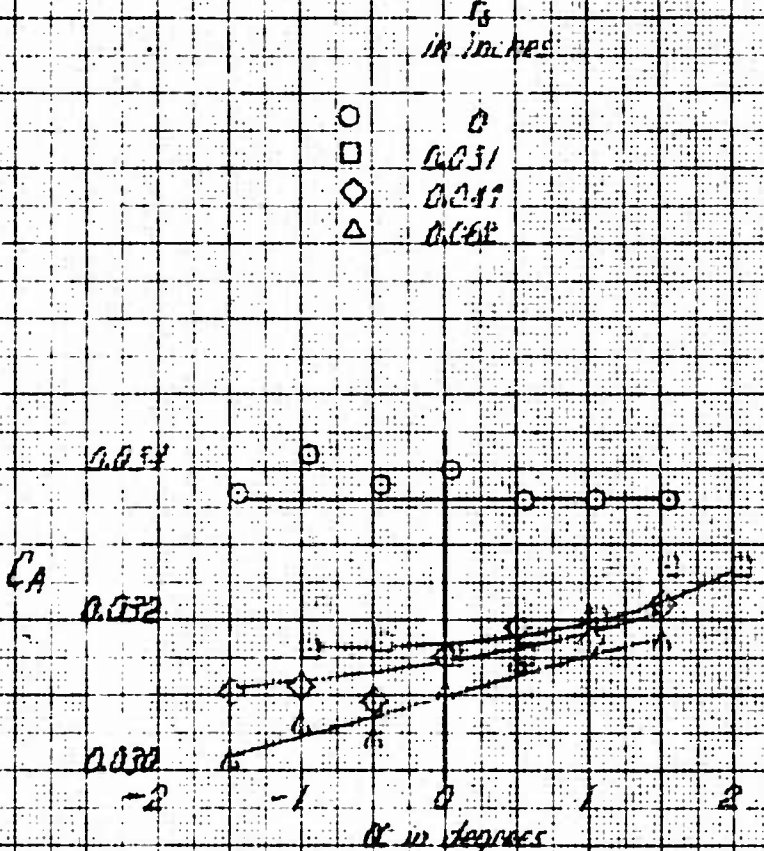

Figure 3 (Concluded)

(b) M = 1.56, Conical Spike Tip, 0.03c Spacing, t = 0.4 inch

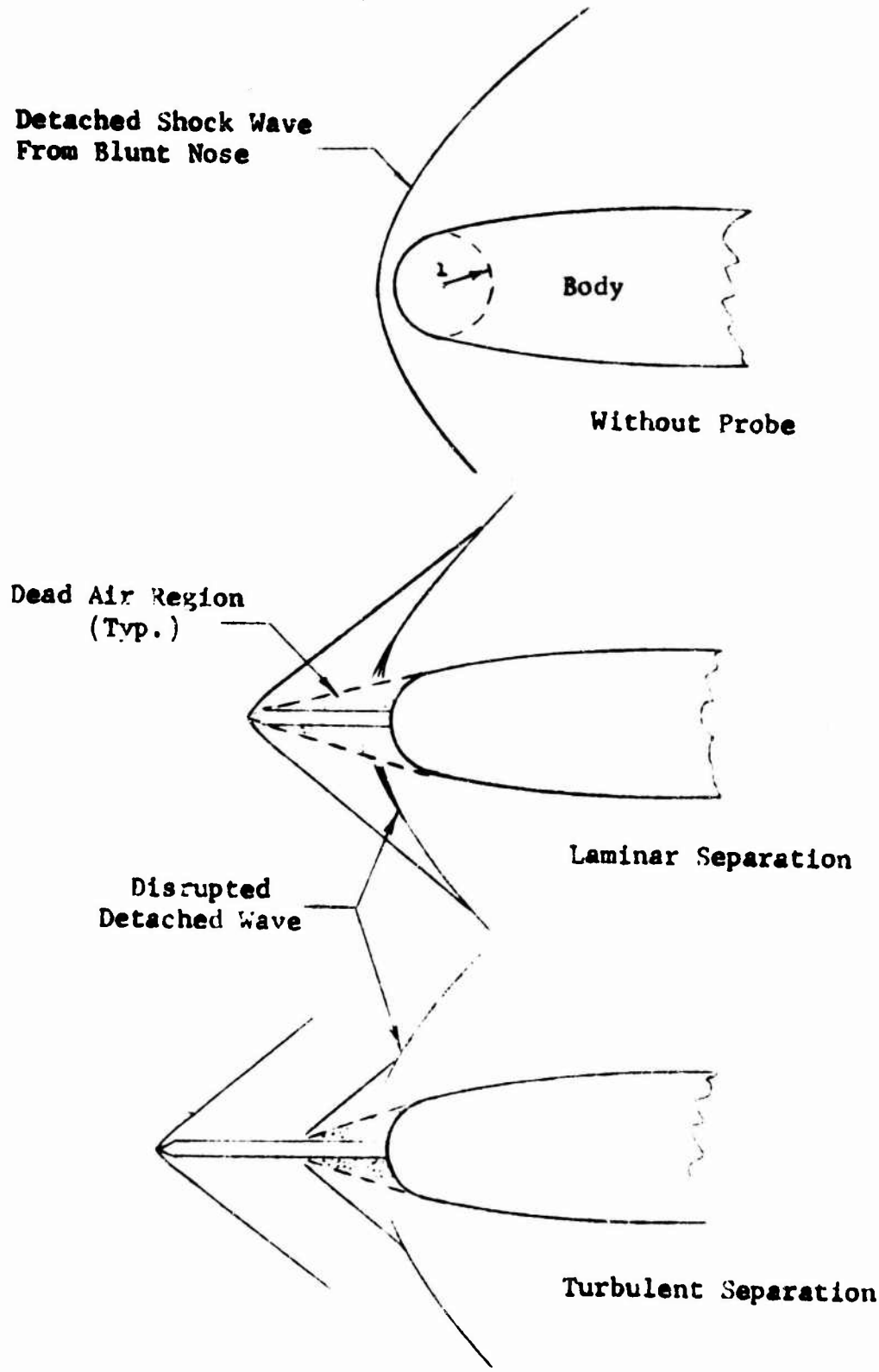

Figure 9 - Flow Phenomena in the Vicinity of Blunt-Nosed Axially-Symmetric Bodies

RH 2 Aug '57

FIGURE 9

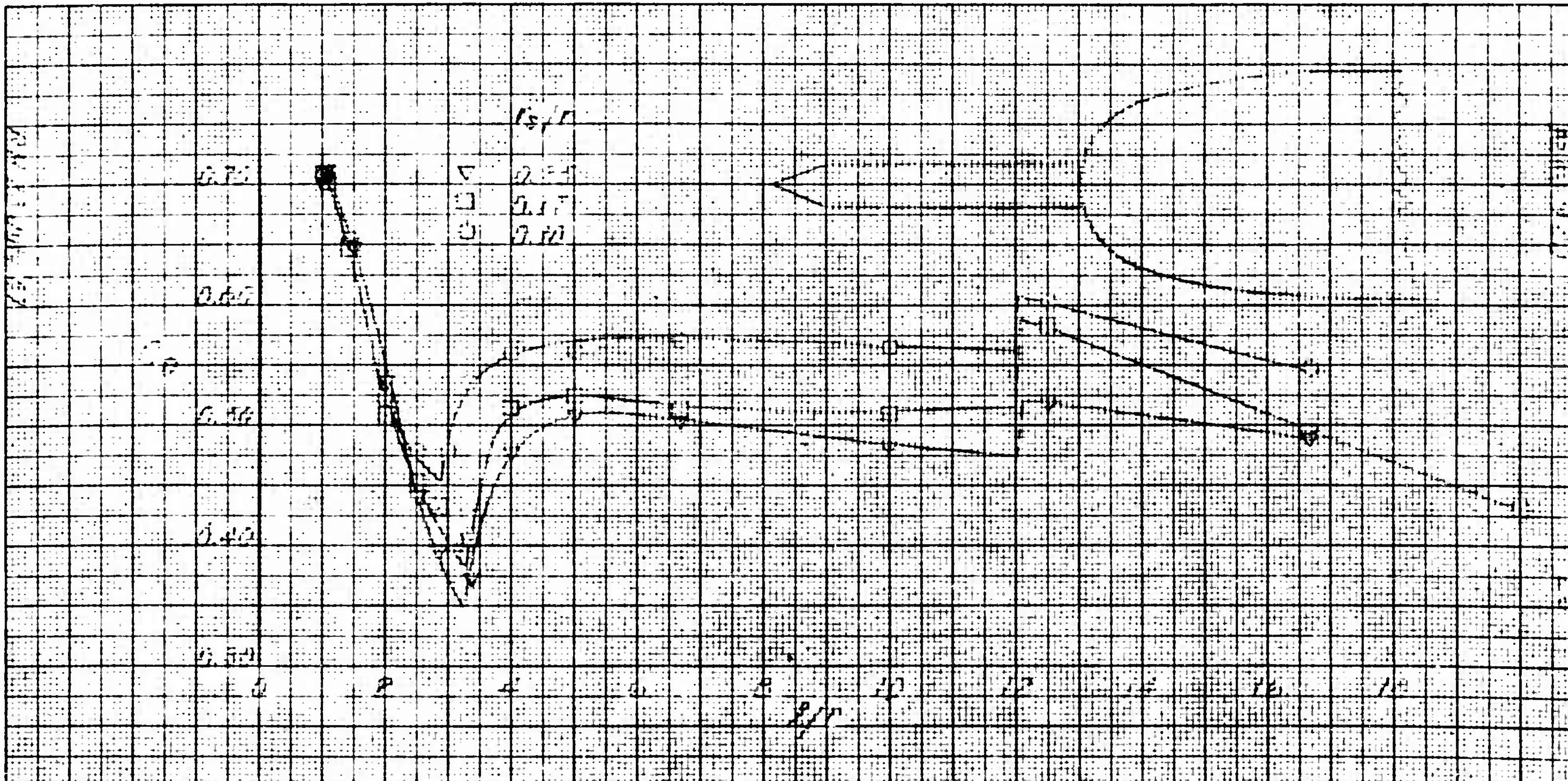

Figure 10 - Drag Reduction From Spikes Placed in Front of Axially-Symmetric Bodies

(a) Data From NACA RM E51F25, M = 1.95

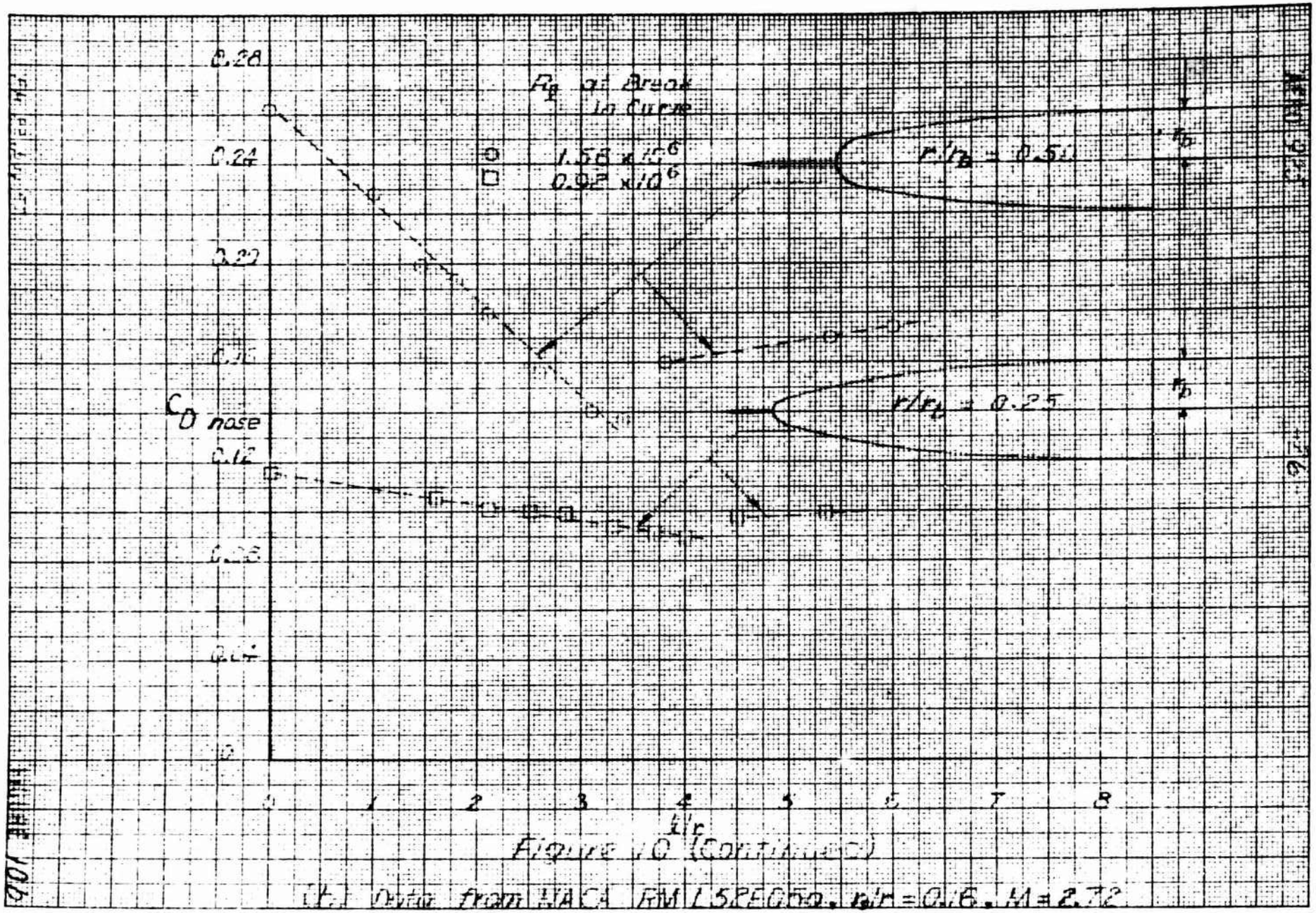

FIGURE 10 (CONTINUED)

[b.] Data from NACA RM L52E05a. $a/r = 0.6$, $M = 2.72$

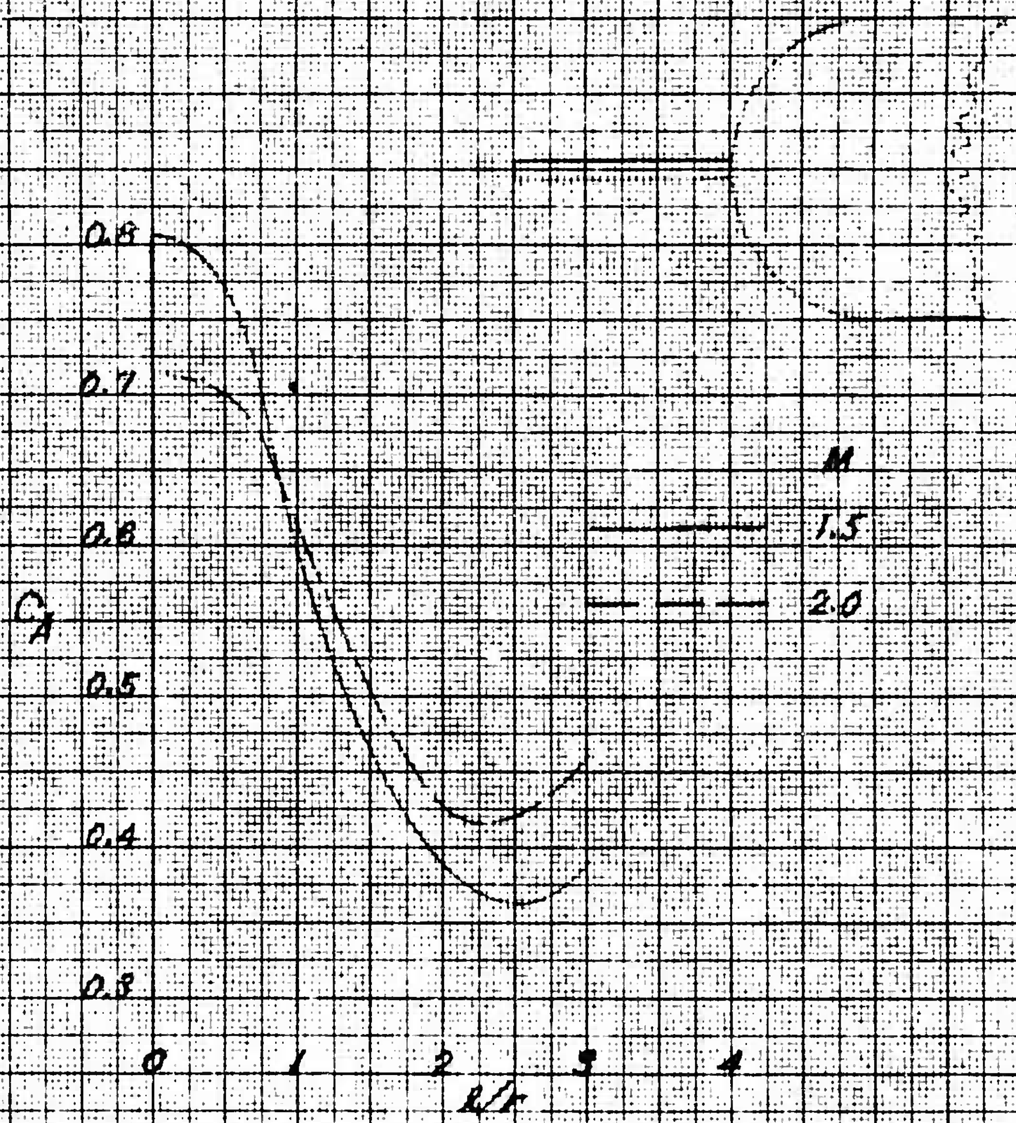

Figure [illegible] (Concluded)

[illegible] $= $ [illegible]

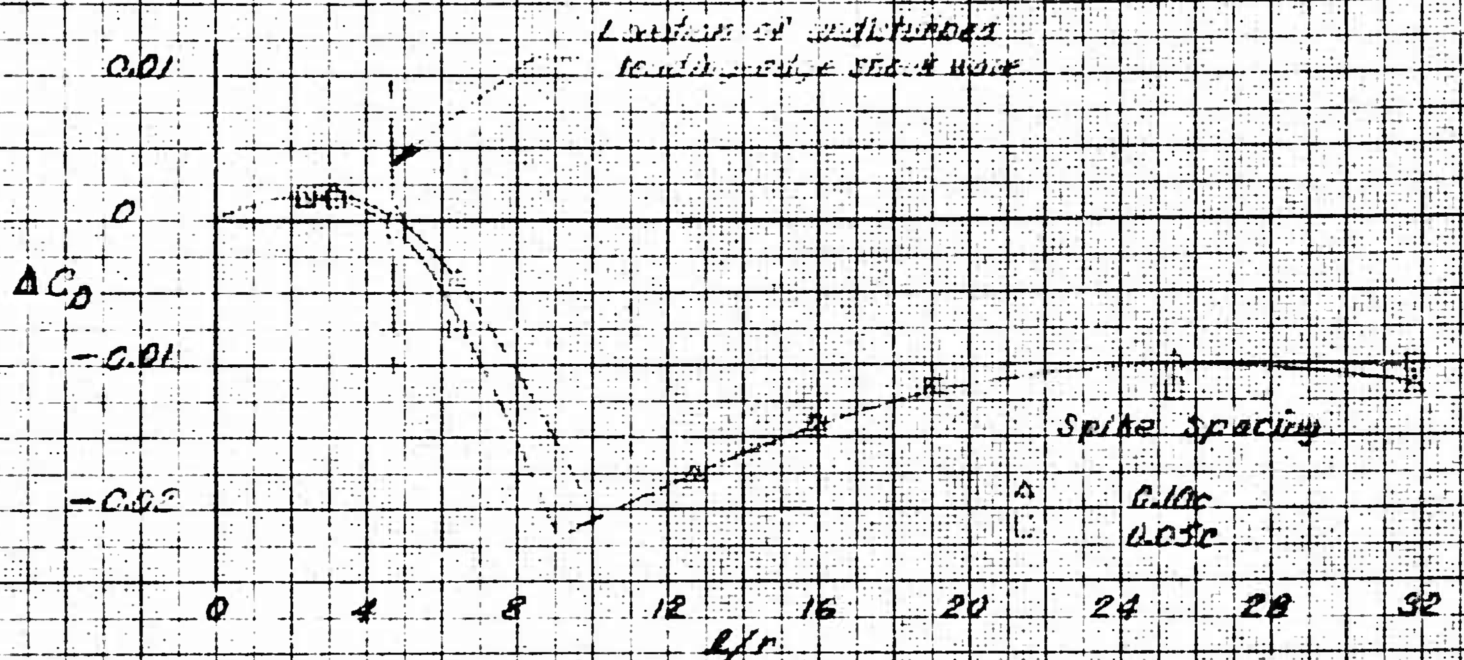

Figure 11.- Effect of Geometric Parameter, ℓ/r, on Incremental Drag-Force Coefficient for 12-Percent-Thick Wing

(a) M = 1.93, Conical Spikes, r = 0.031 inch

FIGURE 11a

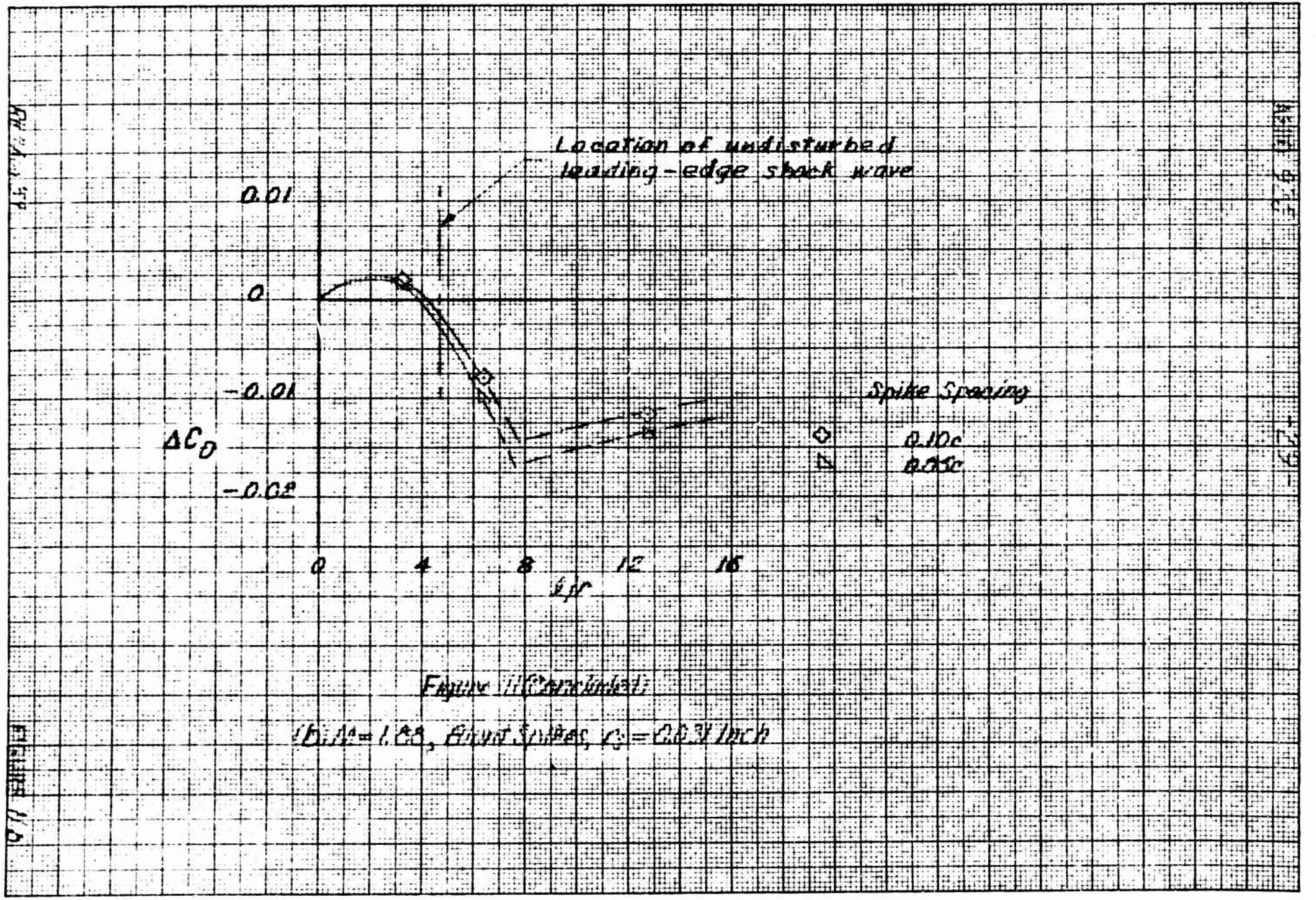

Figure 11.(Concluded)

(b) $M_\infty = 1.68$, Blunt Spikes, $r_s = 0.031$ inch

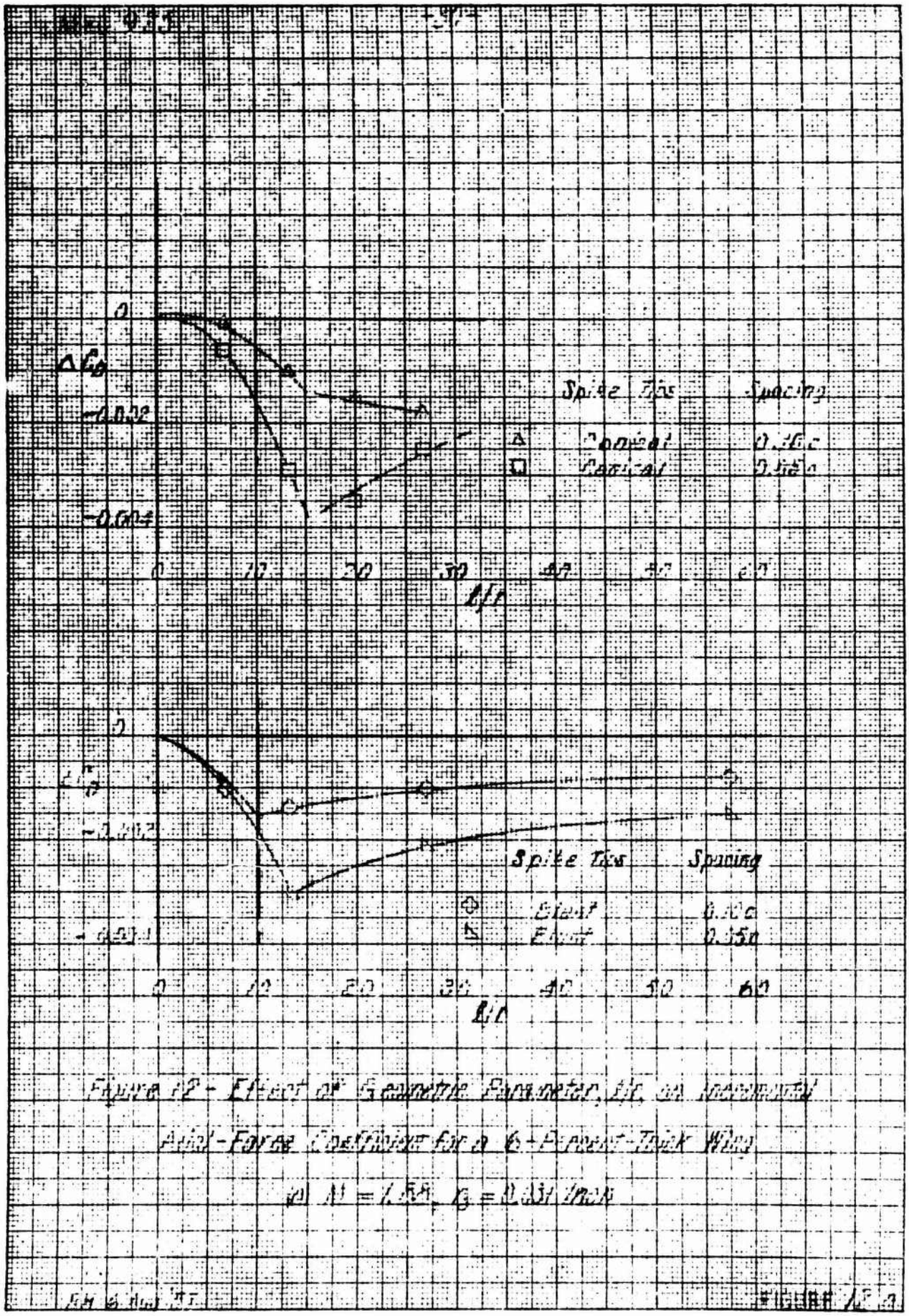

Figure 12 - Effect of Spanwise Separation, L/t, on Incremental Axial-Force Coefficient for a 6-Percent-Thick Wing at M = 1.50, α_B = 0 deg (Ref. 6)

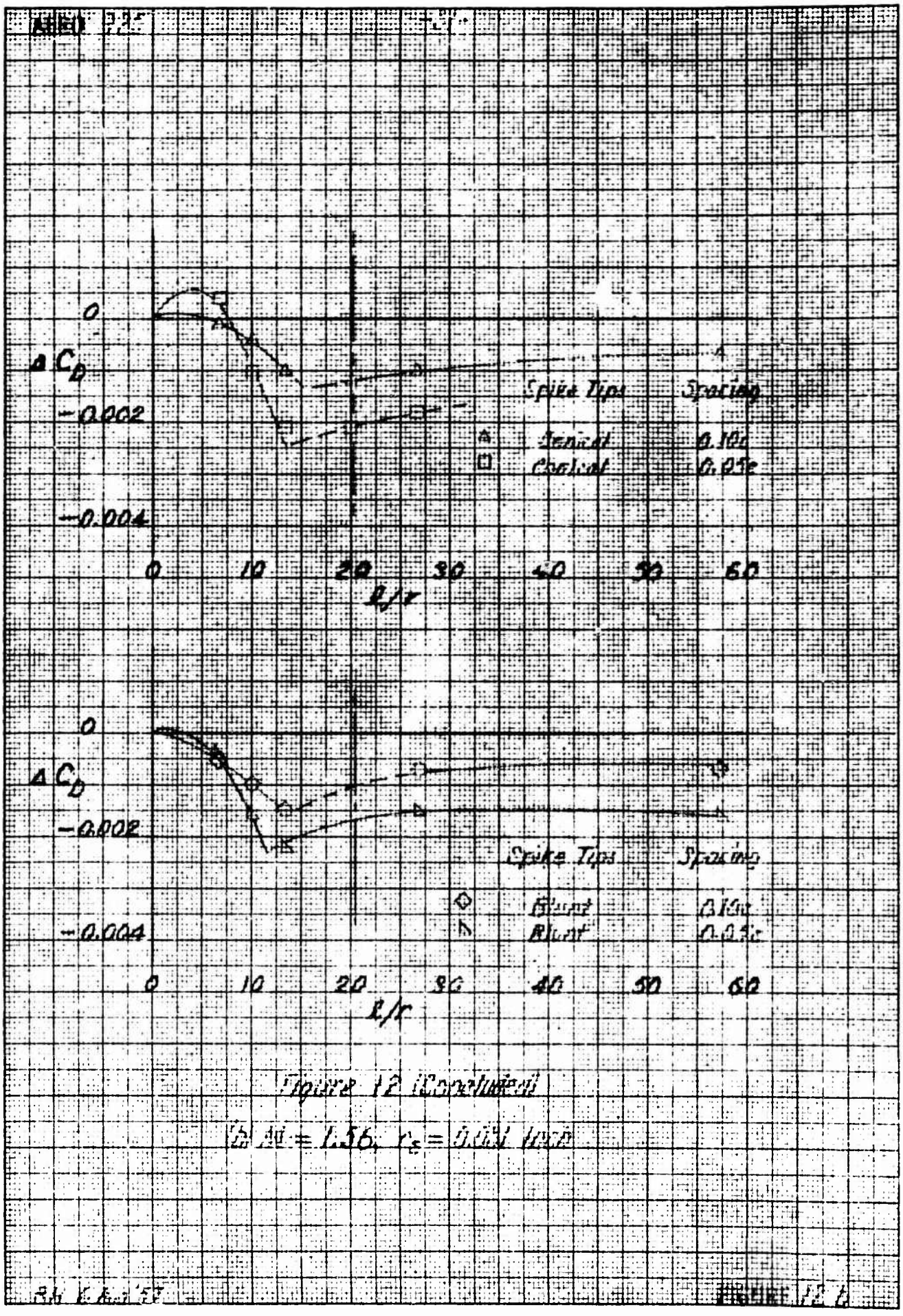

Figure 12 (Continued)

(b) $M = 1.56$, $r_c = 0.04$ inch

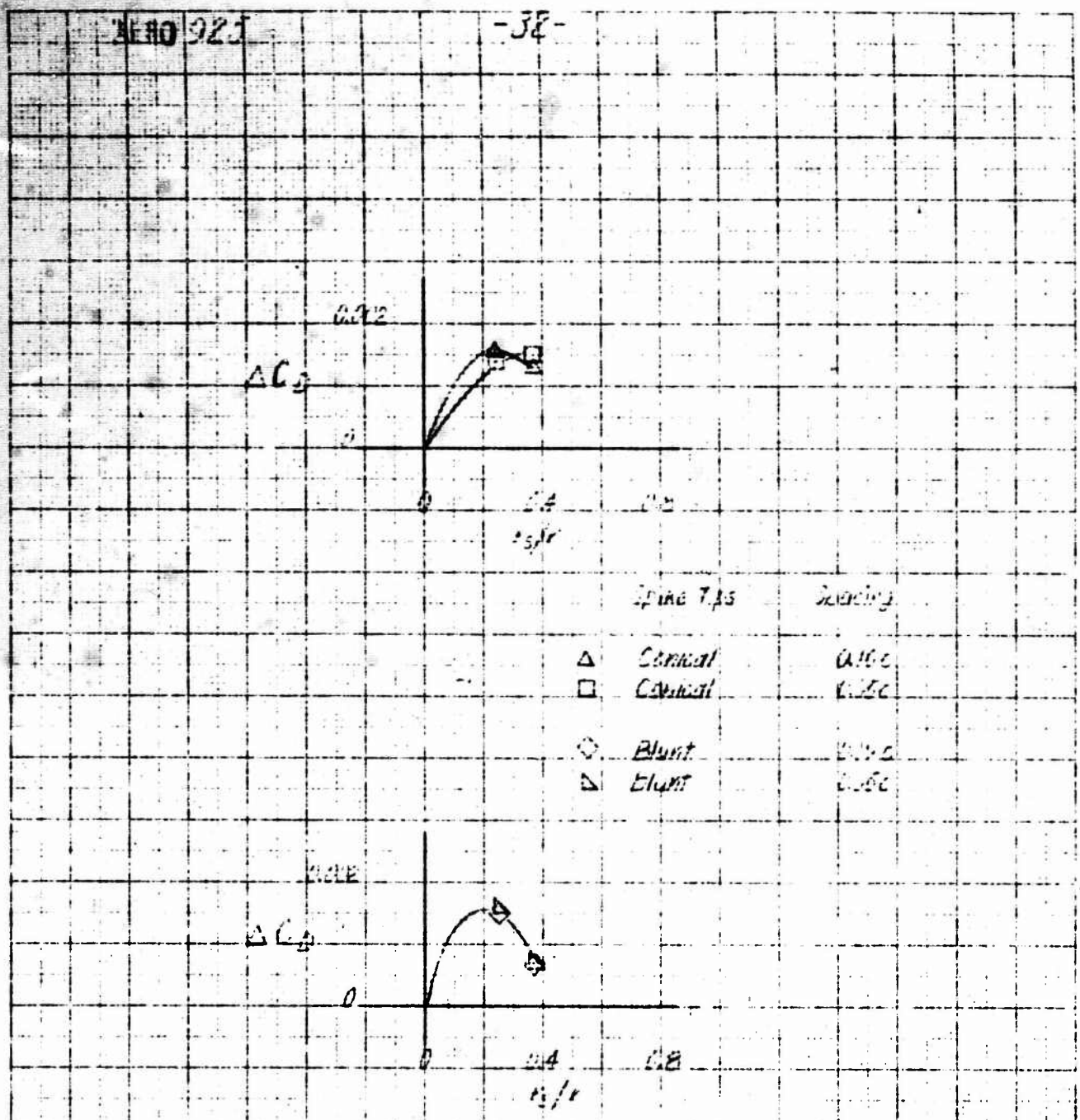

Figure 13 - Effect of Geometric Parameter, r_s/r, on Incremental Axial-Force Coefficient for a 12 Percent Thick Wing

$M = 1.60$, $\ell = 0.4$ inch

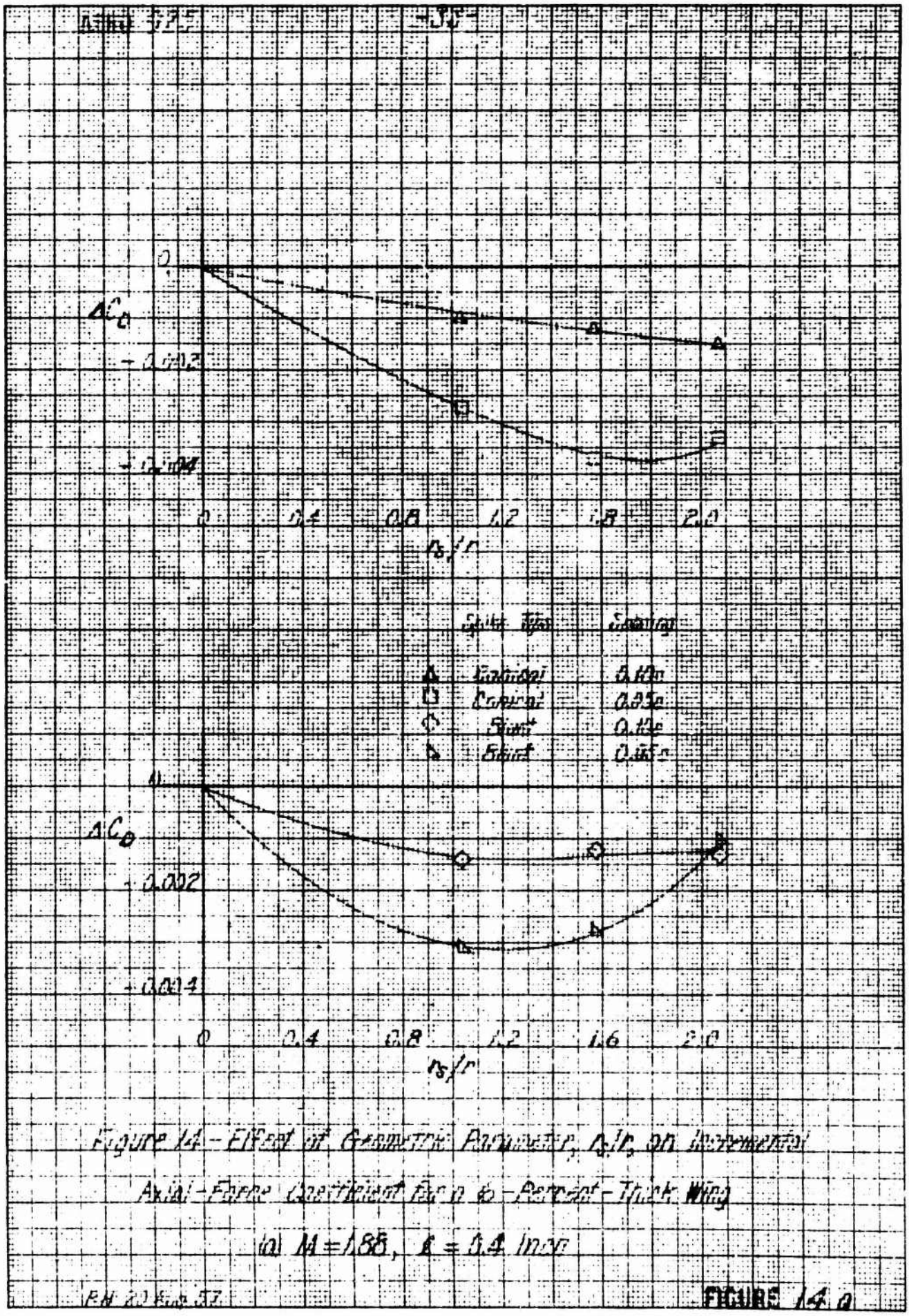

Figure 14 - Effect of Geometric Parameter, r_s/r, on Increment in Axial-Force Coefficient for a 6-Percent-Thick Wing

(a) $M = 1.85$, $k = 0.4$ inch

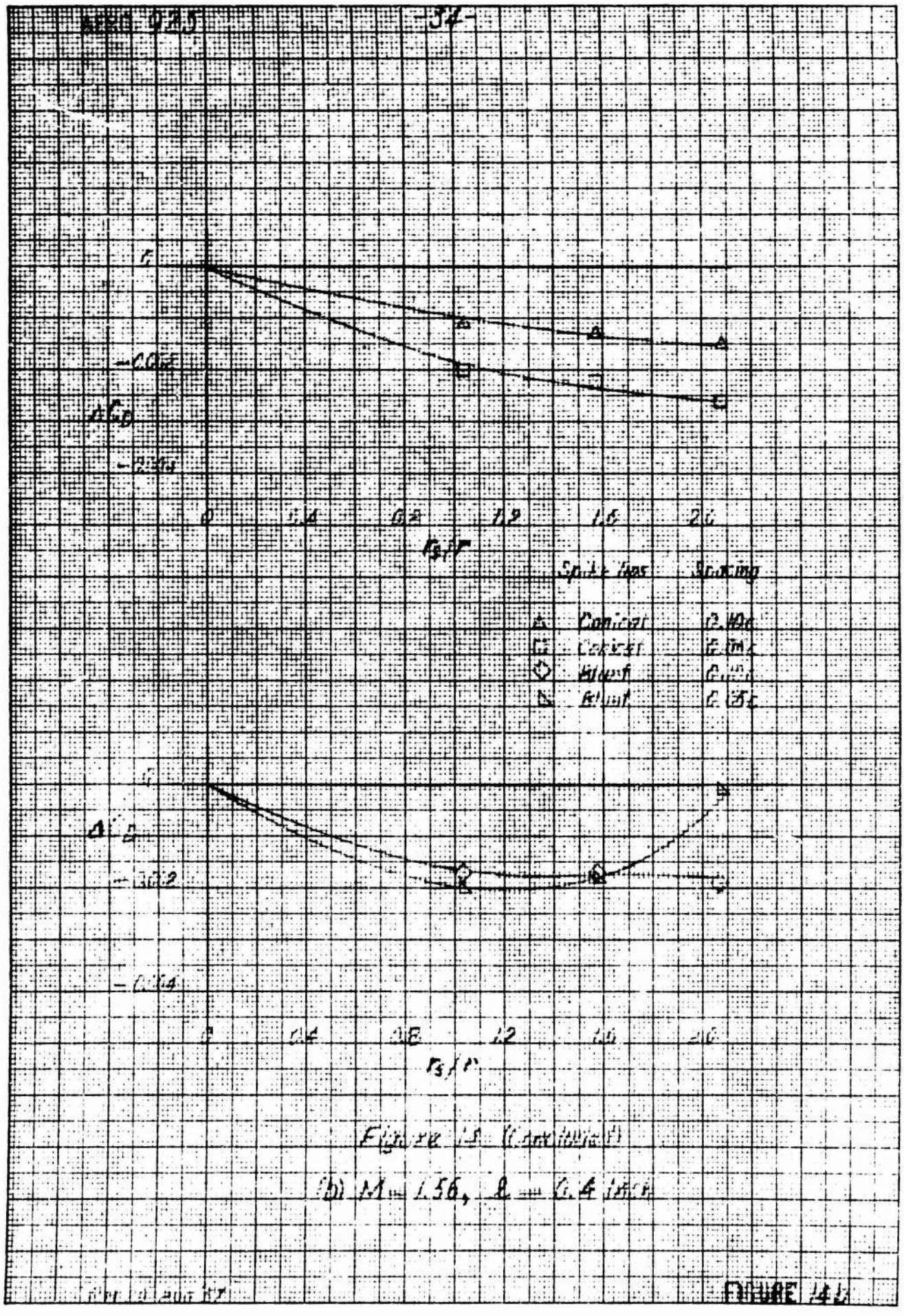

Figure 15 (continued)

(b) $M = 1.56$, $\alpha = 0.4$ deg.

FIGURE 14 b